

Frequency Control Through Voltage Regulation of Power System Using SVC Devices

Mohammed Ahsan Adib Murad, *Student Member, IEEE*, Georgios Tzounas, *Student Member, IEEE*,
Muyang Liu, *Student Member, IEEE*, and Federico Milano, *Fellow, IEEE*
School of Electrical and Electronic Engineering, University College Dublin, Ireland
{mohammed.murad, georgios.tzounas, muyang.liu}@ucdconnect.ie, federico.milano@ucd.ie

Abstract—This paper focuses on voltage-based frequency control by means of Static Var Compensators (SVCs). An additional frequency control loop based on a droop and a PI control is integrated to the voltage control of the SVC to exploit primary frequency control. To illustrate the performance of the combined voltage-frequency controller the WSCC 9-bus and a detailed all-island dynamic model of the Irish system is utilized. The latter shows that frequency-voltage control through shunt FACTS devices can be effective in real-world applications.

Index Terms—Frequency control, Flexible AC Transmission System (FACTS), Static Var Compensator (SVC), voltage control.

I. INTRODUCTION

A. Motivation

The high penetration of renewable energy sources (RES) leads to reduce system inertia as well as frequency regulation. The low inertia is a consequence of the non-synchronous nature of most RES, which are typically connected to the grid through power electronic converters. The reduction of frequency regulation is a consequence of the small or null power reserve with which RES are generally operated as well as of their stochastic behavior, e.g., wind and solar energy. There is thus a clear need of novel solutions to provide frequency support to the grid [1], [2]. With this aim, this paper focuses on the effectiveness of Static Var Compensators (SVCs) to provide fast frequency control through the regulation of voltage dependent loads.

B. Literature Review

A recent emerging strategy to provide frequency support through non-conventional devices is demand-side management, e.g., thermostatically controlled loads [3], [4]. A similar, yet, more general approach is the exploitation of the sensitivity of load power consumption to voltage variations [5]. This approach is known as Voltage-based Frequency Control (VFC) and is the main focus of this paper.

VFC solutions proposed in the literature are based on Automatic Voltage Regulators (AVRs) [6] and Under Load Tap Changer Transformers (ULTCs) [7]. AVR-based frequency control requires conventional power plants. ULTCs, on the

other hand, are not effective for primary frequency control due to their slow response. ULTCs are suitable for secondary and/or tertiary control. A fast smart transformer (FST) with VFC capability is discussed in [8]. FSTs, however, are still to be introduced in real-world power systems.

VFC can be also implemented through Flexible AC Transmission System (FACTS) devices. However, there have been very few proposal of FACTS-based VFC so far, as follows. A primary VFC that includes storage is proposed in [9]. In [10], an SVC connected at a synchronous generator bus is considered, with an additional feedback loop for frequency control. Connecting an SVC at a conventional power plant, however, does not appear to be likely in practice. Currently, this loop is aimed at damping low frequency oscillations (0.1–2 Hz). This configuration is widely known as Power Oscillation Damper (POD) [11]. Finally, reference [12] proposes an SVC-based VFC, considering an adaptive control technique based on the definition of Lyapunov function. Compared to [12], this paper considers simpler yet effective implementations of the VFC transfer functions.

C. Contributions

The contributions of the paper are as follows.

- A discussion on the voltage-based frequency control using SVCs with local measurements and conventional controllers, namely, droop and PI transfer functions.
- A thorough comparison of the performance of SVC-based primary frequency control using the IEEE 9-bus system as well as a detailed and realistic model of the all-island Irish transmission system.

For the all-island Irish transmission system, a real-world contingency is considered. This allows testing the actual effectiveness of the SVC frequency support.

D. Organization

The remainder of this paper is organized as follows. Section II presents the principles and models of the voltage-based frequency control using SVC. The effectiveness of the SVC-based frequency control is described using the benchmark 9-bus and the Irish system and compared with the conventional SVC control in Section III. Finally, Section IV draws conclusions and outlines future work directions.

II. VOLTAGE-BASED FREQUENCY CONTROL

A. Voltage Dependency of Loads

Industrial and residential loads are generally modelled as aggregated power consumption in the dynamic analysis of power systems. These aggregated models can be of static or dynamic [13]. A common static model expresses the active and reactive powers as functions of the bus voltage magnitude, as follows:

$$p = p_0 \left(\frac{v_t}{v_{t0}} \right)^{\alpha_p}, \quad (1)$$

$$q = q_0 \left(\frac{v_t}{v_{t0}} \right)^{\alpha_q}, \quad (2)$$

where p and q are the active and reactive power demand; p_0 and q_0 are the rated active and reactive power demand at the rated voltage (v_{t0}) of the bus; α_p and α_q are the voltage exponents of active and reactive power respectively and v_t is the bus voltage magnitude. The exponents α_p and α_q vary depending on the load type [7]. Typical ranges for the exponents are $\alpha_p \in (0.9, 1.7)$ and $\alpha_q \in (1.9, 4)$ [14].

A change in the operation voltage, say Δv , results in the following change in power demand Δp :

$$\Delta p = ((v_t + \Delta v)^{\alpha_p} - v_t^{\alpha_p}) \frac{p_0}{v_{t0}^{\alpha_p}}. \quad (3)$$

For example, assume $v_t = v_{t0} = 1$ pu and $\alpha_p = 1.5$. Then, a 5% voltage increase will lead to an increase of the active power demand by about 7.6%. The VFC scheme considered in this paper exploits (3) to vary the active power consumption through the variation of the bus voltage magnitudes. Throughout the remainder of the paper, $\alpha_p = 1.5$ and $\alpha_q = 2$ are assumed.

B. Conventional SVC model

An SVC is a combination of a capacitor and a variable shunt reactor controlled through a thyristor-based power electronic switches. The SVC can generate and absorb reactive power and thus is conventionally utilized for voltage control at the bus to which it is connected. The control diagram of an SVC is shown in Fig. 1, where the controlled variable is the susceptance b_{SVC} .

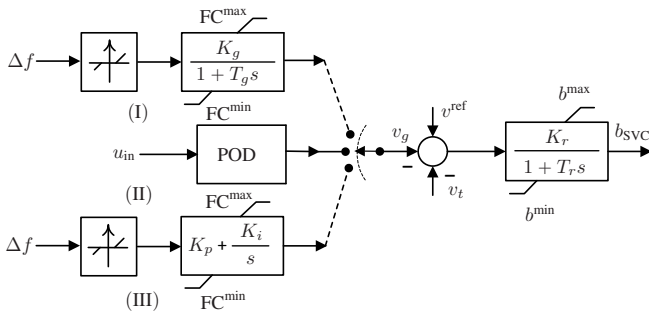


Fig. 1: Block diagram of conventional SVC model with additional control loops: (I) droop frequency control, (II) POD control and (III) PI based frequency control.

The SVC model is defined by the following differential-algebraic equations [13]:

$$T_r \dot{b}_{SVC} = -b_{SVC} + K_r (v^{\text{ref}} - v_t - v_g), \quad (4)$$

$$q = b_{SVC} v_t^2, \quad (5)$$

where v^{ref} , K_r , T_r and q are the reference voltage, the regulator gain, the regulator time constant and the output reactive power generated by the SVC, respectively. In conventional application, the signal v_g is usually the output of a POD.

C. Frequency Control Through SVC

The POD typically used to obtain v_g in Fig. 1, utilizes the rate of change of the input signal u_{in} and serves for damping electro-mechanical oscillations. Instead, we employ two different types of controllers to get v_g , which are designed to achieve VFC.

With this aim, two control methods are considered: (i) a droop (lag) controller and (ii) a Proportional Integral (PI) controller (see (I) and (III) in Fig. 1). For both types the frequency error (Δf) is considered as control input. The presence of the deadband (db) ensures that for a small variation of the frequency, the controller will not deteriorate the local voltage response.

In case that the droop controller is used, v_g is given by:

$$T_g \dot{v}_g = K_g \Delta f - v_g, \quad (6)$$

where T_g and K_g are the time constant and gain of the lag controller, respectively; Δf is the frequency error, where $\Delta f = f^{\text{ref}} - f_i$; f^{ref} is the reference frequency and f_i is the measured frequency at the SVC bus.

If the PI controller were to be used, v_g is as follows:

$$\begin{aligned} v_g &= K_p \Delta f + x_f, \\ \dot{x}_f &= K_i \Delta f, \end{aligned} \quad (7)$$

where K_p , K_i and x_f are the proportional gain, the integral gain and the state variable of the PI control, respectively.

To ensure that the bus voltage remains within its operational range, both types of frequency control constrain the output signal to its respective limits (FC^{max} and FC^{min}). Moreover, anti-windup type limits are considered to get better overall transient response [15].

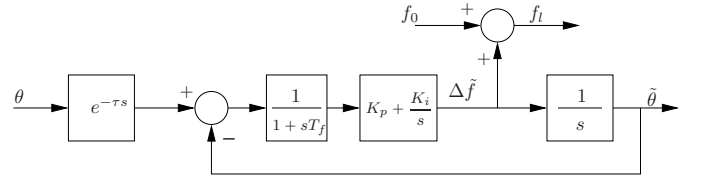


Fig. 2: Lag-PLL block diagram.

In order to obtain the bus frequency f_i , a Phase-Locked Loop (PLL) is utilized. We make use of the Lag-PLL model (see Fig. 2), which produces accurate bus frequency estimations [16]. In Fig. 2, the time required to obtain the bus phase angle (θ) measurement is expressed through a constant delay

block. The error between the measured and estimated phase angle is first passed through a low-pass filter, which reduces the sensitivity of the device to measurement noises. The output is fed to a PI controller, which produces the estimation of the bus frequency deviation ($\Delta\tilde{f}$). The frequency estimation f_l is obtained if the fundamental frequency of the system (f_0) is added to $\Delta\tilde{f}$.

III. CASE STUDIES

The IEEE WSCC 9-bus and the all-island Irish transmission system are considered to study the performance of the examined SVC controls. Based on the discussion in Section II, four scenarios are tested and compared by carrying non-linear time domain simulations: (a) without SVC (NSVC); (b) only conventional ($v_g = 0$) SVC (CSVC); (c) CSVC with lag frequency controller (LFC); and (d) CSVC with PI frequency controller (PIFC).

All simulation results are obtained using Dome, a Python-based software tool for power system analysis [17].

A. WSCC 9-bus System

We consider an SVC connected at bus 8 of the WSCC 9-bus test system shown in Fig. 3. The test network consists of 3 Synchronous Generators (SGs), 3 transformers, 3 loads and 6 transmission lines. All generators are equipped with Automatic Voltage Regulators (AVRs) and Turbine Governors (TGs). The dynamic data of this test network are provided in [18]. The parameters used for the SVC controllers are given in Table I.

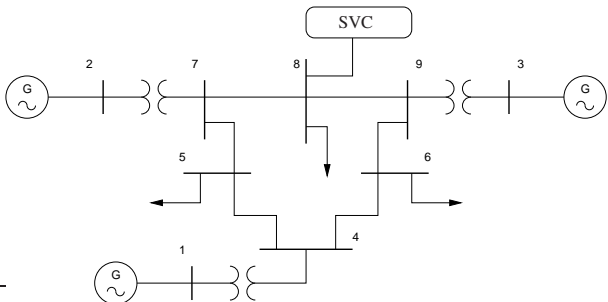


Fig. 3: WSCC 9-bus system with an SVC connected at bus 8.

TABLE I
SVC AND PLL PARAMETERS FOR 9-BUS SYSTEM

Name	Values
CSVC	$K_r = 20, T_r = 0.01, b^{\max} = 0.5 \text{ pu}, b^{\min} = -0.5 \text{ pu}$
LFC	$K_g = 25, T_g = 0.01, db = 0.015 \text{ Hz}, FC^{\text{lim}} = \pm 0.05$
PIFC	$K_p = 1.5, K_i = 25, db = 0.015 \text{ Hz}, FC^{\text{lim}} = \pm 0.05$
PLL	$K_p = 0.1, K_i = 0.5$

1) *Simulation results:* The 9-bus system was simulated by applying a three phase fault at bus 6 at $t = 1$ s. The fault is cleared after 60 ms by tripping the line that connects buses 6 and 9. The trajectories of the frequency of the center of inertia (COI), as well as the voltage at bus 8 are depicted in Figs. 4 and 5, respectively.

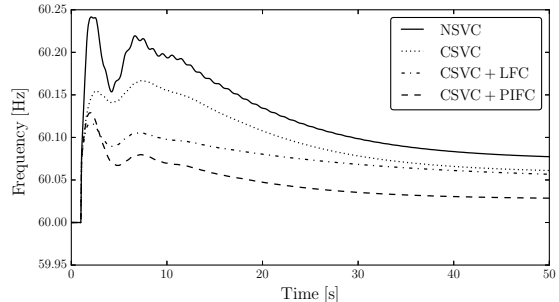


Fig. 4: The frequency response in COI frame.

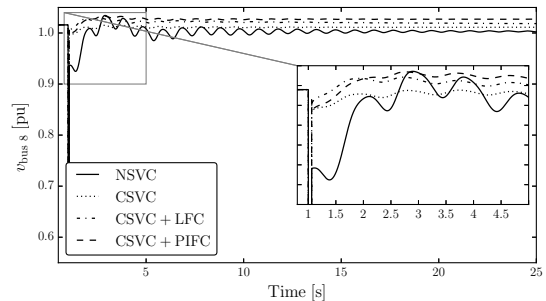


Fig. 5: Response of the voltage at bus 8.

Figure 4 shows that the utilization of LFC and PIFC leads to a significant improvement of the initial frequency deviation. Concerning the voltage response (see Fig. 5), after the disturbance the CSVC provides reactive power support and therefore, improves the bus voltage. This also leads to increase the load consumption, as imposed by (3). In this case, the CSVC leads to a relatively good frequency response even without frequency control loop. But this results is not always guaranteed. How effective is the CSVC for frequency control depends on the disturbance and cannot be determined *a priori*.

No secondary frequency control through automatic generation control is considered in this study. Hence, the trajectories of frequency reach a post disturbance equilibrium with a nonzero steady state error. Compared to all other cases the this error is less when the PIFC is employed. The PIFC also leads to a higher steady state voltage magnitude at the bus of the SVC. This is a consequence of the perfect tracking behavior of the PI control. Note that the PIFC integrator does not eliminate the steady-state frequency error, due to the deadband in the VFC input and the limits on the output.

Overall, the amount of frequency response improvement obtained in Fig. 4 when either LFC or PIFC is included is significant (> 0.1 Hz). It is clear that this improvement varies depending on several factors: size of the system, number of SVCs installed, location of the SVCs etc. To better quantify the real impact of the VFC provided by SVCs, in the next section, we study the effect of inclusion of frequency control loops in the SVCs that the Irish system operator has planned to install in 2019.

B. All-island Irish System

The Irish network is built based on the static data provided by EirGrid Group, the Irish transmission system operator (TSO). Dynamic data are defined based on power plant capacities and technologies [19]. The system consists of 1,479 buses, 1,851 transmission lines and transformers, 245 loads, 22 SGs with AVRs and TGs, 6 Power System Stabilizers (PSSs), 173 wind generators of which 139 are doubly-fed induction generators and 34 are constant speed wind turbines.

1) *Validation of the Irish System:* In order to carry out a realistic case study, we first validate the Irish test system by applying a real severe high frequency event. On 28th February 2018, the VSC-HVDC link East-West Inter-connector (EWIC) [20] that connects the Irish transmission system with the Great Britain (GB) transmission system, was tripped. At that moment, Ireland was exporting 470 MW to GB. Due to the loss of the EWIC, the frequency in the Irish grid rose to 50.42 Hz. Over frequency protections were triggered and several wind farms were curtailed.

In our test system model, we consider the 470 MW active power export as a constant load. A comparison of simulated and actual frequency response following the outage of the EWIC is shown in Fig. 6. With a proper tuning of TG parameters, we managed to obtain a satisfactory match between the simulated transient and the actual one.

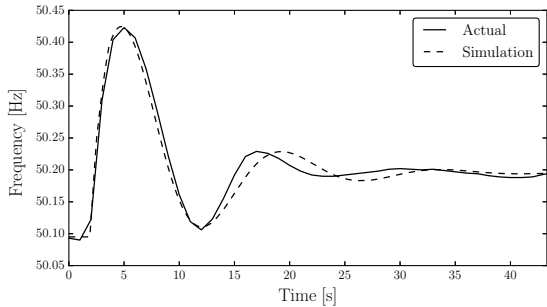


Fig. 6: Comparison of simulated and actual frequency responses due to the loss of the EWIC.

For the purpose of the model validation discussed above, no VFC is considered. In the next section, the frequency response of the Irish system model with inclusion of SVC-based VFC is examined. The same four scenarios discussed for the WSCC 9-bus system are considered.

2) *Set up of SVCs:* The current Irish transmission system includes several shunt capacitors and shunt reactors but only two SVCs for reactive power compensation. The installed SVCs have a capability of +90 and -10 Mvar and are installed at the 110 kV voltage level (see Table B-7 in [21]). Three more SVCs are expected to be integrated at the same voltage level in 2019. The capacity of the new SVCs is ± 470 Mvar (see Table B-11 in [21]).

For our simulations, we have connected all five SVCs at the actual/expected buses and have imposed their limits based on their nominal ratings. The parameters of the SVC controllers

TABLE II
PARAMETERS OF THE SVCs AND PLLS

Name	Values
CSVC	$K_r = 25, T_r = 0.01$
LFC	$K_g = 75, T_g = 0.005, db = 0.015$ Hz
PIFC	$K_p = 1.5, K_i = 50, db = 0.015$ Hz
PLL	$K_p = 0.1, K_i = 0.5$

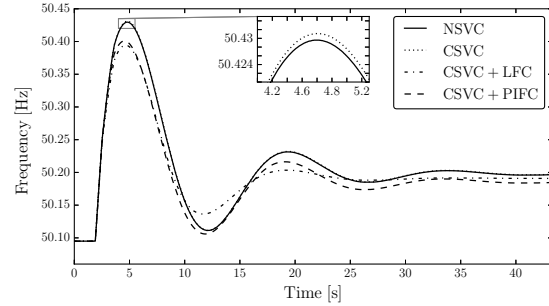


Fig. 7: Response of the frequency due to the loss of the EWIC.

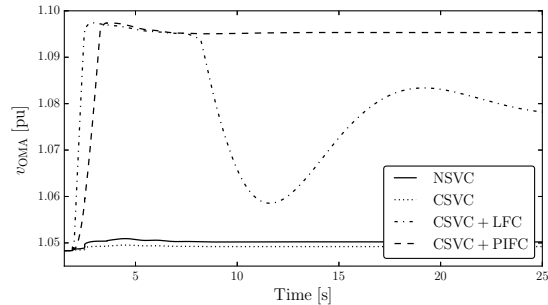


Fig. 8: Response of the voltage at bus Omagh Main due to the loss of the EWIC.

and the PLLs are given in Table II. Except for reactive power limits, all parameters are the same for the five SVCs.

3) *Contingency I:* The test system is simulated by applying the disturbance discussed in Section III-B1. The comparative trajectories of the frequency and the voltage at an SVC bus (Omagh Main) are shown in Figs. 7 and 8, respectively. The NSVC case is same as the simulated response shown in Fig. 6. Compared to NSVC and CSVC, the utilization of CSVC with LFC and PIFC improves the frequency response. This improvement (for LFC ≈ 0.037 Hz and for PIFC ≈ 0.03 Hz) is relevant given that only 5 SVCs are utilized.

At the time of the EWIC outage, the active power generation in the Irish system is greater than the demand. Hence, the bus voltage is increased by the SVC with LFC and PIFC to increase power consumption. On the other hand, the CSVC without frequency control ensures the best voltage control, which in turn slightly deteriorates the frequency response (see zoomed view in Fig. 7). Due to the limits imposed in the VFC, voltage fluctuations remain within the maximum operating range (1.1 pu). Even though PIFC provides the minimum steady-state error, the overall transient response of the frequency is better when the LFC is used.

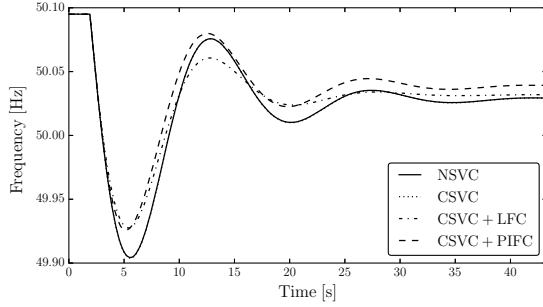


Fig. 9: Response of the frequency due to the loss of 155 MW generation.

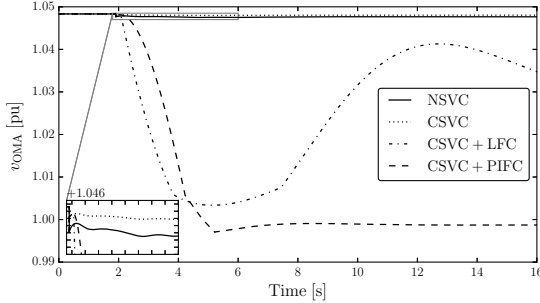


Fig. 10: Response of the voltage at bus Omagh Main due to the loss of 155 MW generation.

4) *Contingency II*: The previous section discusses an event that leads to over-frequency transient. For completeness, we now consider losing a part of the generation, which leads to an under-frequency transient response. In particular, we assume that 155 MW of generation is disconnected. The results for the four examined scenarios are shown in Figs. 9 and 10. An overall better response is achieved with compared to NSVC and CSVC cases. The voltage also remains well within its lower bound (0.9 pu).

C. Discussion

In all scenarios considered in this case study, the SVCs are connected at a transmission level. This solution is the most flexible from the point of view of the TSOs because it does not require that they engage with customers or distribution system operators. Moreover, no VFC strategy discussed in the paper requires changing the existing infrastructure or to develop a communication framework. This is an added value of the proposed VFC based on SVCs. Even if the TSOs wanted to limit the utilization of SVCs exclusively for voltage control in normal operation, the VFC could be enabled following a large contingencies. This can be achieved safely and automatically by simply setting a large db value in the input of the VFC.

IV. CONCLUSIONS

This paper studies voltage-based frequency control provided by SVCs. The proposed VFC schemes utilize exclusively local voltage and frequency measurements. Simulation results indicate that even a small number of SVCs can effectively support the primary frequency control without worsening the voltage response of a large network.

It is important to note that the effectiveness of the VFC heavily relies on load models. Future work will dedicate on modeling realistic system load composition and then quantify the amount of virtual reserve can be provided by the SVCs.

REFERENCES

- [1] F. Milano, F. Dörfler, G. Hug, D. J. Hill, and G. Verbič, "Foundations and challenges of low-inertia systems (invited paper)," in *2018 Power Systems Computation Conference (PSCC)*, June 2018, pp. 1–25.
- [2] B. Kroposki, B. Johnson, Y. Zhang, V. Gevorgian, P. Denholm, B. Hodge, and B. Hannegan, "Achieving a 100% renewable grid: Operating electric power systems with extremely high levels of variable renewable energy," *IEEE Power and Energy Magazine*, vol. 15, no. 2, pp. 61–73, March 2017.
- [3] E. Vrettos, C. Ziras, and G. Andersson, "Fast and reliable primary frequency reserves from refrigerators with decentralized stochastic control," *IEEE Transactions on Power Systems*, vol. 32, no. 4, pp. 2924–2941, July 2017.
- [4] I. Beil, I. Hiskens, and S. Backhaus, "Frequency regulation from commercial building HVAC demand response," *Proceedings of the IEEE*, vol. 104, no. 4, pp. 745–757, April 2016.
- [5] A. Moeini and I. Kamwa, "Analytical concepts for reactive power based primary frequency control in power systems," *IEEE Transactions on Power Systems*, vol. 31, no. 6, pp. 4217–4230, Nov 2016.
- [6] M. Farrokhabadi, C. A. Cañizares, and K. Bhattacharya, "Frequency control in isolated/islanded microgrids through voltage regulation," *IEEE Transactions on Smart Grid*, vol. 8, no. 3, pp. 1185–1194, 2017.
- [7] A. Ballanti, L. N. Ochoa, K. Bailey, and S. Cox, "Unlocking new sources of flexibility: Class: The world's largest voltage-led load-management project," *IEEE Power and Energy Magazine*, vol. 15, no. 3, pp. 52–63, 2017.
- [8] G. De Carne, G. Buticchi, M. Liserre, and C. Vournas, "Load control using sensitivity identification by means of smart transformer," *IEEE Transactions on Smart Grid*, vol. 9, no. 4, pp. 2606–2615, July 2018.
- [9] M. T. Holmberg, M. Lahtinen, J. McDowall, and T. Larsson, "SVC Light[®] with energy storage for frequency regulation," in *IEEE Conference on Innovative Technologies for an Efficient and Reliable Electricity Supply*, 2010, pp. 317–324.
- [10] A. El-Emary and M. El-Shibina, "Application of static var compensation for load frequency control," *Electric machines and power systems*, vol. 25, no. 9, pp. 1009–1022, 1997.
- [11] ABB FACTS Division, "A matter of FACTS deliver more high quality power," Product Guide, ABB, 2015.
- [12] Y. Wan, M. A. A. Murad, M. Liu, and F. Milano, "Voltage frequency control using SVC devices coupled with voltage dependent loads," *IEEE Transactions on Power Systems*, pp. 1–1, 2018.
- [13] F. Milano, *Power System Modelling and Scripting*, ser. Power Systems. Springer Berlin Heidelberg, 2010.
- [14] A. J. Collin, G. Tsagarakis, A. E. Kiprakis, and S. McLaughlin, "Development of low-voltage load models for the residential load sector," *IEEE Transactions on Power Systems*, vol. 29, no. 5, pp. 2180–2188, Sept 2014.
- [15] M. A. A. Murad, Á. Ortega, and F. Milano, "Impact on power system dynamics of PI control limiters of VSC-based devices," in *2018 Power Systems Computation Conference (PSCC)*, June 2018, pp. 1–7.
- [16] Á. Ortega and F. Milano, "Comparison of different PLL implementations for frequency estimation and control," in *Procs. of the 18th International Conference on Harmonics and Quality of Power (ICHQP)*, May 2018, pp. 1–6.
- [17] F. Milano, "A Python-based software tool for power system analysis," in *IEEE PES General Meeting*, Vancouver, BC, 2013, pp. 1–5.
- [18] P. M. Anderson and A. A. Fouad, *Power System Control and Stability*. Wiley-IEEE Press, 2003.
- [19] Á. Ortega and F. Milano, "Modeling, simulation, and comparison of control techniques for energy storage systems," *IEEE Transactions on Power Systems*, vol. 32, no. 3, pp. 2445–2454, May 2017.
- [20] J. Egan, P. O'Rourke, R. Sellick, P. Tomlinson, B. Johnson, and S. Svensson, "Overview of the 500MW EirGrid East-West Interconnector, considering system design and execution-phase issues," in *Universities Power Engineering Conference (UPEC)*, Sept 2013, pp. 1–6.
- [21] EirGrid and SONI, "All-Island Ten Year Transmission Forecast Statement 2016," Tech. Rep., 2017.